Ethylene Oligomerization with Cr−NHC Catalysts: Further Insights into the Extended Metallacycle Mechanism of Chain Growth

David S. McGuinness,*[,†] James A. Suttil,[†] Michael G. Gardiner,[†] and Noel W. Davies[‡]

School of Chemistry, University of Tasmania, Private Bag 75, Hobart, Tasmania 7001, Australia, and Central Science Laboratory, University of Tasmania, Private Bag 74, Hobart, Tasmania 7001, Australia

Received May 4, 2008

The mechanism of ethylene oligomerization with chromium(III) complexes of bis(carbene)pyridine ligands in combination with MAO has been investigated. Oligomerization with mixtures of CH_2CH_2/CD_2CD_2 reveals that this system produces α-olefins via an extended metallacycle mechanism. Deviation form a Schulz−Flory distribution has been explained on the basis of less favorable product release at the early stages of metallacycle growth ($Cr-C_4$ ($\pm Cr-C_6$)). Significant amounts of branched olefins (methylidenes) and linear internal olefins are produced at the high catalyst loadings employed in this study, and these result from secondary incorporation of α-olefins into the metallacycle mechanism. Changing the ligand C^N^C coordination mode in any way resulted in a sharp loss of activity. In the case of bidentate carbene−pyridine and carbene−thiophene ligands, this is due to a change in the mechanism from metallacycle to linear chain growth. Thus, only those catalysts which support a metallacycle mechanism promote oligomerization with high activity.

1. Introduction

The commercial oligomerization of ethylene is predominately carried out using transition-metal or alkylaluminum catalysts which produce a broad distribution of linear α-olefins (LAOs). Around half of the LAOs produced are employed as comonomers for the production of linear low density polyethylene (LLDPE copolymers), which utilizes the 1-butene, 1-hexene, and 1-octene fractions.[1] Increasing demand from the polymer industry for 1-hexene and 1-octene has therefore led LAO producers to seek more selective oligomerization technologies in which the production of less valuable, or lower volume olefins, can be largely avoided. The selective trimerization of ethylene to 1-hexene[2−13] and the more recent tetramerization to 1-octene[14−25] are such processes which are currently the focus of much attention.

The mode of selective 1-hexene and 1-octene generation relies on a metallacyclic mechanism (Scheme 1). The key to the selectivity of these systems appears to be the energetically preferred tendency of $M-C_6$ and $M-C_8$ metallacycles to undergo a product releasing β-hydrogen shift rather than further ethylene insertion.[25−30] At the same time, a constrained

* To whom correspondence should be addressed. E-mail: david.mcguinness@utas.edu.au.

† School of Chemistry.

‡ Central Science Laboratory.

(1) *Eur. Chem. News***2004**, *80*, 16.

(2) Dixon, J. T.; Green, M. J.; Hess, F. M.; Morgan, D. H. *J. Organomet. Chem.* **2004**, *689*, 3641.

(3) Deckers, P. J. W.; Hessen, B.; Teuben, J. H. *Angew. Chem., Int. Ed.* **2001**, *40*, 2516.

(4) Andes, C.; Harkins, S. B.; Murtuza, S.; Oyler, K.; Sen, A. *J. Am. Chem. Soc.* **2001**, *123*, 7423.

(5) Carter, A.; Cohen, S. A.; Cooley, N. A.; Murphy, A.; Scutt, J.; Wass, D. F. *Chem. Commun.* **2002**, 858.

(6) McGuinness, D. S.; Wasserscheid, P.; Keim, W.; Hu, C.; Englert, U.; Dixon, J. T.; Grove, C. *Chem. Commun.* **2003**, 334.

(7) McGuinness, D. S.; Wasserscheid, P.; Keim, W.; Morgan, D. H.; Dixon, J. T.; Bollmann, A.; Maumela, H.; Hess, F.; Englert, U. *J. Am. Chem. Soc.* **2003**, *125*, 5272.

(8) Morgan, D. H.; Schwikkard, S. L.; Dixon, J. T.; Nair, J. J.; Hunter, R. *Adv. Synth. Catal.* **2003**, *345*, 1.

(9) Köhn, R. D.; Smith, D.; Mahon, M. F.; Prinz, M.; Mihan, S.; Kociok-Köhn, G. *J. Organomet. Chem.* **2003**, *683*, 200.

(10) Wu, T.; Qian, Y.; Huang, J. *J. Mol. Catal. A* **2004**, *214*, 227.

(11) Bluhm, M. E.; Walter, O.; Döring, M. *J. Organomet. Chem.* **2005**, *690*, 713.

(12) de Wet-Roos, D.; Dixon, J. T. *Macromolecules* **2004**, *37*, 93414.

(13) Blann, K.; Bollmann, A.; Dixon, J. T.; Hess, F.; Killian, E.; Maumela, H.; Morgan, D. H.; Neveling, A.; Otto, S.; Overett, M. *Chem. Commun.* **2005**, 620.

(14) Bollmann, A.; Blann, K.; Dixon, J. T.; Hess, F. M.; Killian, E.; Maumela, H.; McGuinness, D. S.; Morgan, D. H.; Neveling, A.; Otto, S.; Overett, M.; Slawin, A. M. Z.; Wasserscheid, P.; Kuhlmann, S. *J. Am. Chem. Soc.* **2004**, *126*, 14712.

(15) Overett, M. J.; Blann, K.; Bollmann, A.; Dixon, J. T.; Haasbroek, D.; Killian, E.; Maumela, H.; McGuinness, D. S.; Morgan, D. H. *J. Am. Chem. Soc.* **2005**, *127*, 10723.

(16) Overett, M. J.; Blann, K.; Bollmann, A.; Dixon, J. T.; Hess, F. M.; Killian, E.; Maumela, H.; Morgan, D. H.; Neveling, A.; Otto, S. *Chem. Commun.* **2005**, 622.

(17) Walsh, R.; Morgan, D. H.; Bollmann, A.; Dixon, J. T. *App. Catal. A* **2006**, *306*, 184.

(18) Kuhlmann, S.; Dixon, J. T.; Haumann, M.; Morgan, D. H.; Ofili, J.; Spuhl, O.; Taccardi, N.; Wasserscheid, P. *Adv. Synth. Catal.* **2006**, *348*, 1200.

(19) Elowe, P. R.; McCann, C.; Pringle, P. G.; Spitzmesser, S. K.; Bercaw, J. E. *Organometallics* **2006**, *25*, 5255.

(20) Jabri, A.; Crewdson, P.; Gambarotta, S.; Korobkov, I.; Duchateau, R. *Organometallics* **2006**, *25*, 715.

(21) McGuinness, D. S.; Overett, M.; Tooze, R. P.; Blann, K.; Dixon, J. T.; Slawin, A. M. Z. *Organometallics* **2007**, *26*, 1108.

(22) Rucklidge, A. J.; McGuinness, D. S.; Tooze, R. P.; Slawin, A. M. Z.; Pelletier, J. D. A.; Hanton, M. J.; Webb, P. B. *Organometallics* **2007**, *26*, 2782.

(23) McGuinness, D. S.; Rucklidge, A. J.; Tooze, R. P.; Slawin, A. M. Z. *Organometallics* **2007**, *26*, 2561.

(24) Kuhlmann, S.; Blann, K.; Bollmann, A.; Dixon, J. T.; Killian, E.; Maumela, M. C.; Maumela, H.; Morgan, D. H.; Prétorius, M.; Taccardi, N.; Wasserscheid, P. *J. Catal.* **2007**, *245*, 279.

(25) Janse van Rensburg, W.; van den Berg, J.-A.; Steynberg, P. J. *Organometallics* **2007**, *26*, 1000.

(26) de Bruin, T. J. M.; Magna, L.; Raybaud, P.; Toulhoat, H. *Organometallics* **2003**, *22*, 3404.

(27) Tobisch, S.; Ziegler, T. *Organometallics* **2003**, *22*, 5392.

(28) Blok, A. N. J.; Budzelaar, P. H. M.; Gal, A. W. *Organometallics* **2003**, *22*, 2564.

(29) Yu, Z.-X.; Houk, K. N. *Angew. Chem., Int. Ed.* **2003**, *42*, 808.

10.1021/om800398e CCC: $40.75
Publication on Web 08/02/2008

Scheme 1. Metallacycle Mechanism of Ethylene Trimerization and Tetramerization

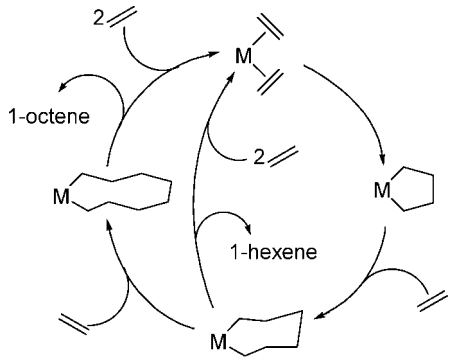

geometry of the metallacycle prevents the β-hydrogen shift reaction at the $M-C_4$ stage and, as such, very low amounts of 1-butene are produced. In 2004, Bercaw and co-workers provided conclusive experimental evidence of a metallacyclic mechanism by way of a series of experiments with deuterated ethylene.[31,32] The simplest of these experiments involves trimerization with a mixture of CH_2CH_2 and CD_2CD_2, which leads to a 1-hexene isotopomer distribution of only C_6H_{12}, $C_6H_8D_4$, $C_6H_4D_8$, and C_6D_{12}. The lack of H/D scrambling observed strongly indicates a metallacycle mechanism and is inconsistent with a Cossee−Arlman linear chain growth mechanism. This experiment represents a relatively straightforward method of distinguishing between the two mechanisms and has subsequently been used to show that ethylene tetramerization to 1-octene also occurs via a metallacycle mechanism.[15]

While most interest in metallacyclic oligomerization revolves around its ability to very selectively produce 1-hexene and 1-octene, a further interesting aspect is the possibility of growth to large ring metallacycles, leading to a distribution of higher olefins and ultimately polyethylene. This situation would come about when the energy barrier to further insertion and metallacycle growth (at the $M-C_6$ and $M-C_8$ stage) is comparable or lower than the barrier for product elimination. The most active trimerization and tetramerization catalysts are based upon Cr, so it is perhaps not surprising that the first experimental confirmation of large ring metallacyclic oligomerization and polymerization was found for homogeneous Cr catalysts. Gibson and co-workers recently reported a number of chromium catalysts which give a mathematical distribution of α-olefins via metallacycle growth, as demonstrated by deuterium-labeling studies.[33,34] These findings are relevant to ongoing debate about the mechanism of polymerization with heterogeneous Phillips Cr/silica type catalysts. These catalysts have been used on great industrial scale over many years; however, despite this the mechanism of chain growth is still highly uncertain.[35,36] Extended metallacycle growth has been discussed as a strong possibility.[37−39]

Given the industrial importance of Cr-based oligomerization and polymerization catalysts, it is of interest to further investigate the occurrence of the extended metallacycle mechanism. A number of highly active Cr oligomerization catalysts which give Schulz−Flory distributions of LAOs are known,[40−43] raising the question of how general the metallacycle mechanism is in these systems and in Cr-based polymerization catalysts in general. Identifying whether a particular catalyst operates via a linear chain growth or a metallacycle mechanism is of more than academic interest. In principle, a metallacycle mechanism offers the potential of catalyst tuning toward lighter $C_{2n}H_{4n}$ oligomers (trimerization and tetramerization), without concomitant 1-butene formation. This is not possible when a Cossee−Arlman mechanism is operating, as a shift to lower carbon numbers necessarily increases the percentage of 1-butene.

In 2003, one of us reported Cr-based ethylene oligomerization precatalysts **1** and **2** which incorporate CNC-pincer carbene ligands.[43,44] Once activated with MAO, these complexes formed exceptionally active catalysts for Schulz−Flory oligomerization to LAOs and low molecular weight polymer, with TOFs in ethylene over 10^6 h^{-1} being achievable under optimal conditions. Herein we have revisited these systems in order to elucidate the mechanism of chain growth and to investigate the effects of ligand modification on olefin selectivity. The mechanism of chain growth is shown to be ligand dependent, with high activity resulting only in cases where a metallacycle mechanism has been demonstrated.

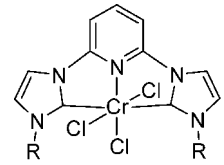

1 R=^{i}Pr
2 R=2,6-^{i}Pr$_2$C$_6$H$_3$

2. Results and Discussion

2.1. Mechanism of Chain Growth. It was previously reported[43,44] that chromium complexes **1** and **2** are highly active for ethylene oligomerization, giving a Schulz−Flory distribution of LAOs when activated with MAO. The distribution of oligomers, characterized by the K value,[45] was lower for **1** (0.46−0.48) than for **2** (0.75−0.80). The activity of both is approximately first order in ethylene, and the value of K is independent of ethylene pressure in the range from 1−5 bar, indicating that both chain propagation and chain transfer are first order in ethylene.

Oligomerization with **1** and **2** was carried out with a mix of CD_2CD_2 and CH_2CH_2 at 1 bar total pressure in a stirred Schlenk flask. The products were analyzed by GC−MS showing that each oligomeric peak was made up predominately of even numbered isotopomers (D_0, D_4, D_8...). The 1-decene fraction

(30) Janse van Rensburg, W.; Grove, C.; Steynberg, J. P.; Stark, K. B.; Huyser, J. J.; Steynberg, P. J. *Organometallics* **2004**, *23*, 1207.
(31) Agapie, T.; Schofer, S. J.; Labinger, J. A.; Bercaw, J. E. *J. Am. Chem. Soc.* **2004**, *126*, 1304.
(32) Agapie, T.; Labinger, J. A.; Bercaw, J. E. *J. Am. Chem. Soc.* **2007**, *129*, 14281.
(33) Tomov, A. K.; Chirinos, J. J.; Jones, D. J.; Long, R. J.; Gibson, V. C. *J. Am. Chem. Soc.* **2005**, *127*, 10166.
(34) Tomov, A. K.; Chirinos, J. J.; Long, R. J.; Gibson, V. C.; Elsegood, M. R. J. *J. Am. Chem. Soc.* **2006**, *128*, 7704.
(35) Groppo, E.; Lamberti, C.; Bordiga, S.; Spoto, G.; Zecchina, A. *Chem. Rev.* **2005**, *105*, 115.
(36) Theopold, K. H. *Eur. J. Inorg. Chem.* **1998**, 15.
(37) Zielinski, P.; Dalla Lana, I. G. *J. Catal.* **1992**, *137*, 368.
(38) Ruddick, V. J.; Badyal, J. P. S. *J. Phys. Chem. B* **1998**, *102*, 2991.
(39) Espelid, Ø.; Børve, K. J. *J. Catal.* **2002**, *206*, 331.
(40) Döhring, A.; Göhre, J.; Jolly, P. W.; Kryger, B.; Rust, J.; Verhovnik, G. P. J. *Organometallics* **2000**, *19*, 388.
(41) Döhring, A.; Jensen, V. R.; Jolly, P. W.; Thiel, W.; Weber, J. C. *Organometallics* **2001**, *20*, 2234.
(42) Small, B. L.; Carney, M. J.; Holman, D. M.; O'Rourke, C. E.; Halfen, J. A. *Macromolecules* **2004**, *37*, 4375.
(43) McGuinness, D. S.; Gibson, V. C.; Wass, D. F.; Steed, J. W. *J. Am. Chem. Soc.* **2003**, *125*, 12716.
(44) McGuinness, D. S.; Gibson, V. C.; Steed, J. W. *Organometallics* **2004**, *23*, 6288.
(45) $K = k_{\text{propagation}}/(k_{\text{propagation}} + k_{\text{chain transfer}}) = \text{mol of } C_{n+2}/\text{mol of } C_n$.

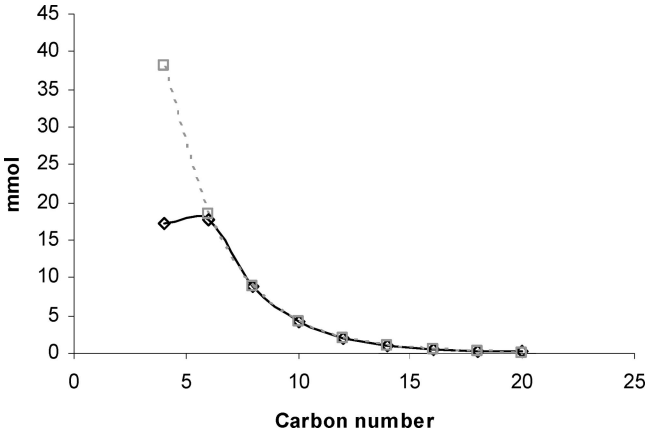

Figure 1. Plot of the molar amount of oligomers formed versus carbon number (C_4-C_{20}) for (a) the catalyst system **1** (10 μmol), 500 equiv of MAO, 50 mL of toluene, 5 bar of ethylene, 30 min (black line); (b) the calculated distribution for a K value of 0.48 (gray line).

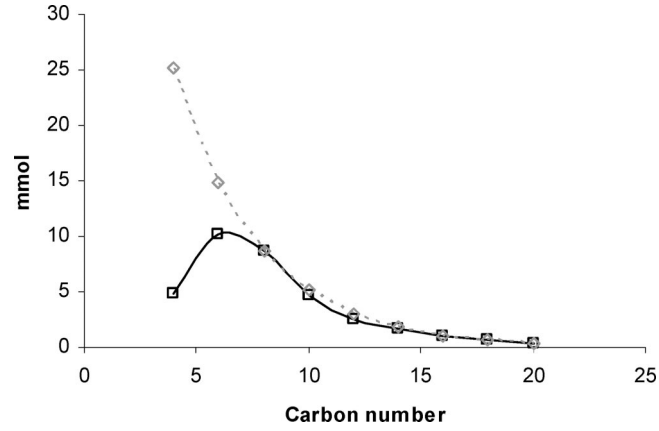

Figure 2. Plot of the molar amount of oligomers formed versus carbon number (C_4-C_{20}) for (a) the catalyst system **2** (10 μmol), 500 equiv of MAO, 50 mL of toluene, 5 bar of ethylene, 25 °C, 30 min (black line); (b) the calculated distribution for a K value of 0.59 (gray line).

was more carefully analyzed, wherein each isotopomer from molecular weight 140 (D_0) to 160 (D_{20}) was quantified. Comparison of the experimental 1-decene distribution with that predicted for a metallacycle mechanism is good for both **1** and **2**,[46] showing that oligomerization occurs via an extended metallacycle mechanism with both catalysts.

2.2. Oligomer Distribution. A perfect Schulz−Flory distribution of oligomers can only result when the rate constants for chain propagation, k_p, and for product release are constant for all chain lengths, which is expected to be approximately the case for a Cossee−Arlman linear chain growth mechanism involving chain transfer (k_{ct}, reaction 1). However, when a metallacycle mechanism is operative the rate of product elimination can be highly dependent on the size of the metallacycle. This is expected to be the case for the smaller metallacycles (Cr−C_4, Cr−C_6, Cr−C_8), and in particular, the Cr−C_4 metallacycle is expected to be the most stable toward elimination of 1-butene.[26−28]

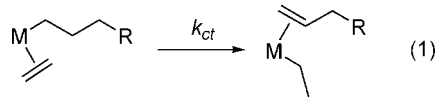

(1)

Having established a metallacycle mechanism for **1** and **2**, we have repeated ethylene oligomerization experiments with these catalysts with the aim of carefully analyzing all oligomeric fractions up to C_{20}. In the previous study of these catalysts, the oligomer distribution was calculated from the C_8-C_{16} fractions only. This is because the more volatile components 1-butene, and possibly 1-hexene, can be partially lost during postcatalysis quenching and off-gassing. In this work, the reactor was cooled to 0 °C prior to bleeding, the ethylene off-gas was collected and its 1-butene content analyzed. Together with analysis of the liquid fraction, this afforded an accurate quantification of both 1-butene and 1-hexene formed during catalysis. Ethylene oligomerization was carried out in toluene using either Albemarle MAO or Akzo-Nobel MMAO-3A, and again analysis of the C_{8+} oligomers closely fits a Schulz−Flory distribution for both **1** and **2**. However, including 1-butene and 1-hexene in the analysis reveals significant deviation from a Schulz−Flory distribution. This is illustrated for catalyst **1** in Figure 1, which compares the actual molar distribution of C_4-C_{20} oligomers with that predicted for a Schulz−Flory distribution with a K value of 0.48. While all oligomers from 1-hexene up closely fit such a distribution, the amount of 1-butene formed is only 45% of that expected; revealing that metallacycle decomposition at the Cr−C_4 stage is significantly retarded relative to ethylene insertion. This is not unexpected, as the almost complete absence of 1-butene formation in ethylene trimerization and tetramerization is well-known. It is perhaps more surprising that any appreciable 1-butene is formed at all, as β-hydride transfer from a metallacyclopentane is expected to be very unfavorable.[26−28] This work shows that it is possible for this process to occur at a rate at least somewhat competitive with further metallacycle expansion.

Activation of **2** with MMAO-3A leads to similar behavior. A Schulz−Flory distribution ($K = 0.78$) is obeyed for the C_6-C_{20} oligomers, while the amount of 1-butene formed is only 48% of that expected. When Albemarle MAO was used to activate **2**, the results differed, however. First, the K value for C_8-C_{20} decreased to 0.59, indicating an increased preference for product release versus metallacycle growth. At the same time, however, both 1-butene and 1-hexene formation is lower than expected based on a Schulz−Flory distribution (Figure 2). The amount of 1-butene formed is only 19% of that predicted, while there is only 69% of the predicted amount of 1-hexene. Evidently, with this cocatalyst both Cr−C_4 and Cr−C_6 metallacycles are relatively stable toward olefin release compared to higher metallacycles. This represents a qualitatively similar bias to that which must exist for ethylene tetramerization catalysts, except in our case higher metallacycle formation is competitive with M−C_8 product release. It has recently been shown that the nature of the cocatalyst can affect C_6/C_8 ratios with ethylene trimerization and tetramerization catalysts,[23] and this has been put down to cocatalyst anion interaction with Cr. Here again, we note the pronounced influence a cocatalyst can have on metallacycle growth and decomposition.

As noted above, the product distribution has been found to be relatively unaffected by changes in the ethylene pressure ($\approx$ concentration), while the activity of the catalysts are approximately first order in ethylene pressure. The observed activity equates to the rate of ethylene insertion, which is reasonably expected to be first order in ethylene.[47] However, the independence of oligomer distribution on ethylene pressure indicates that chain termination from the growing metallacycles is likewise first order in ethylene, which is not as easy to explain.

(46) See the Supporting Information for details.

Scheme 2. Metallacycle Decomposition via (a) an Ethylene-Free Complex and (b) an Ethylene-Coordinated Complex

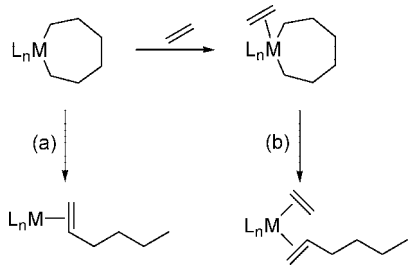

Theoretical mechanistic studies of ethylene trimerization have invariably considered product elimination from metallacycle species lacking any interaction with further ethylene (path a, Scheme 2). Thus, olefin formation should be relatively unaffected by ethylene concentration. This is clearly not the case for the present system, and an ethylene-assisted α-olefin formation must be considered. One possibility which can be postulated is that olefin formation preferentially occurs from an intermediate in which ethylene is coordinated (path b, Scheme 2). Lacking further insight into this process, it is difficult to suggest why this would be the case. It is possible that ethylene coordination could stabilize the transition state to β-hydride transfer, in addition to an expected stabilization of the product complex.

In this context, it is worth discussing some recent findings in ethylene trimerization and tetramerization with Cr−PNP complexes. A number of kinetic studies[17,18] have shown that the rate of oligomerization increases with increasing ethylene concentration, as might be expected. However, the influence of pressure on 1-octene/1-hexene selectivity is much smaller, indicating that increases in ethylene concentration increase the rates of both metallacycle growth and decomposition by comparable amounts (otherwise, a pronounced shift to 1-octene selectivity would be observed upon increasing ethylene concentration). This indicates that 1-hexene formation from the $Cr-C_6$ metallacycle is also promoted by ethylene, similar to the results obtained herein. Recent theoretical studies of the Cr−PNP/MAO tetramerization system are also relevant here.[25] These showed that, within the $Cr-C_6$ metallacycle, ethylene coordination can occur by displacing the MAO anion. Interestingly, this appears to lead to enhanced interaction between a β-hydrogen of the metallacycle and the chromium center. The next step, 1-hexene formation from the ethylene coordinated complex, was not studied, however.

2.3. Formation of Secondary Products from Olefin Incorporation. Our reinvestigation of catalysts **1** and **2** has also revealed that small amounts of branched olefins are detected prior to each main α-olefin peak at relatively high catalyst loadings ([Cr] = 200 μM). Analysis of these by ^{1}H NMR spectroscopy and GC−MS both before and after hydrogenation of the sample afforded identification of the major branched species from $C_{10}-C_{20}$.[46] These products are consistent with incorporation of preformed α-olefins into the metallacycle mechanism, as shown in Scheme 3 (path a or b). The structures indicate that incorporation occurs via either an initial oxidative coupling of ethylene with the α-olefin to yield a metallacyclopentane substituted at the β-carbon, followed by further ethylene insertions into the unsubstituted end of the metallacycle

Scheme 3. Possible Pathways for Higher Olefin Incorporation into the Metallacycle Mechanism

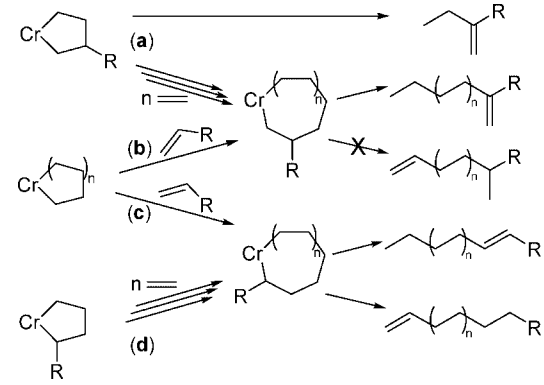

(pathway a), or a 1,2-insertion of the α-olefin into a preformed metallacycle (pathway b). For instance, in a standard oligomerization with **1**, the C_{14} fraction contained 1.4% 7-methylenetridecane (1-octene plus three ethylene units), 2.7% 5-methylenetridecane (1-decene plus two ethylene units), and 3.7% 3-methylenetridecane (1-dodecene plus one ethylene unit). Progressively higher fractions display a greater complexity of peaks, due to the possibility of cooligomerization of ethylene with progressively higher α-olefins, but in each case the major products observed are consistent with only this mode of secondary incorporation.

Branched olefin formation was further investigated by adding 1-pentene to a standard ethylene oligomerization run with catalyst **2**, which gives rise to a minor distribution of odd carbon numbered olefins along with the usual distribution of even carbon numbered olefins. While these odd-numbered olefins are predominately methylidenes arising from pathway a or b, each fraction contains a second minor component which reveals a second mode of incorporation not seen in straight ethylene oligomerization. ^{1}H NMR spectroscopic analysis of the total oligomer mix shows that ca. 3% is made up of internal olefins, and retention indices of the C_9, C_{11}, and C_{13} peaks indicate these minor products are linear olefins with the double bond in the 1-, 3-, or 4-position. These products could arise from either pathway c or d in Scheme 3, followed by β-hydride transfer from either the substituted end of the metallacycle (internal olefin) or the unsubstituted end of the metallacycle (α-olefin). Hydride transfer from the substituted end at the endocyclic β-position would give 4-alkenes when 1-pentene is incorporated in this fashion. These linear α/internal olefins arising from secondary incorporation are not observed in the even carbon numbered fractions, as they are masked by the large α-olefin peaks formed by ethylene homo-oligomerization.[48]

Secondary co-oligomerization of 1-hexene and 1-octene has been reported previously for Cr−PNP ethylene tetramerization catalysts, and in this case, incorporation via a pathway leading to methylidenes was also noted (along with the formation of methyl-branched α-olefins).[15] In contrast, ethylene trimerization catalysts do not appear to lead to methylidenes to any great extent.[32,49] Instead, β-hydrogen transfer occurs preferentially from the unsubstituted end of the metallacycle, generating a methyl-branched α-olefin. In these cases, a much more limited

(47) Theoretical studies on the ethylene trimerization reaction generally show that metallacycle growth (ethylene insertion) is the rate-determining step.[27,28,30]

(48) However, NMR analysis of the product mix resulting from ethylene homo-oligomerization with **2** ([Cr] = 400 μM revealed the sample contained 90% vinyl, 8% methylidene, and 2% internal olefins). See the Supporting Information.

(49) Deckers, P. J. W.; Hessen, B.; Teuben, J. H. *Organometallics* **2002**, *21*, 5122.

Scheme 4. Preparation of Complex 3.

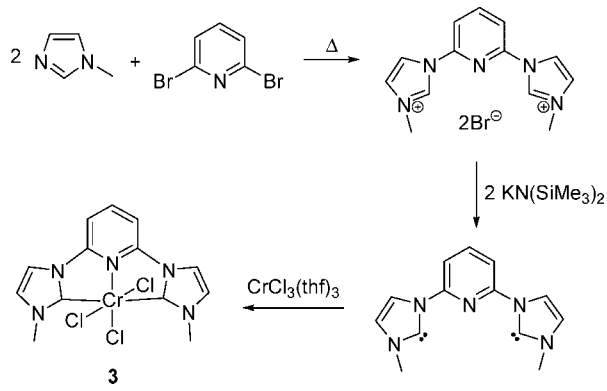

range of products are formed, as only 1-hexene (± 1-octene) is available to co-trimerize (± cotetramerize) with ethylene. In the present case, a distribution of α-olefins are available to co-oligomerize with any number of ethylene units, and hence, an extended range of products results. Gibson and co-workers raised the possibility of incorporation of α-olefins into an extended metallacycle mechanism in their earlier work[33] but concluded that this was not occurring for their catalyst system. To our knowledge, this is the first time secondary incorporation has been observed for an extended metallacycle mechanism and further serves to highlight the similarities between this process and ethylene trimerization/tetramerization.

2.4. Catalyst Ligand Modification. Close similarities exist between catalysts **1** and **2** and known ethylene trimerization and tetramerization catalysts. In addition to oligomerization via a metallacycle mechanism, retarded metallacycle decomposition at the M−C_4 stage (and M−C_6 in the case of **2**) is indicative of some potential for selective trimerization (and tetramerization). With this in mind, we set about modification of the ligands in order to explore the effect this would have on olefin selectivity.

Preparation and Oligomerization Studies of *N*-Methyl-Substituted Cr(C^N^C)Cl_3 (3). Steric bulk on the carbene nitrogen center has been shown to affect the olefin distribution, with complex **1** leading to shorter chain olefins than **2**. Thus, it was hoped that decreasing the steric bulk further might lead to greater selectivity toward the more valuable α-olefins 1-hexene and 1-octene. Complex **3**, containing methyl substitution, was prepared according to Scheme 4 and crystals suitable for an X-ray study were grown by vapor diffusion of methylene chloride into a DMSO solution. The molecular structure of **3** is shown in Figure 3 and displays a distorted octahedral geometry with the tridentate ligand in a meridonal arrangement. Distortion from an ideal octahedral geometry is caused by the tight N−Cr−C chelate bite angles [75.76(7)°] as was observed in the structure of **1** (corresponding angles of 76.3(2) and 75.68(9)°).[43] The Cr−C/N bond distances are as expected and likewise very similar to those observed in **1**. As such, changing the *N*-substituents from isopropyl in **1** to methyl in **3** has not caused any significant changes in the coordination geometry of the complex.

Similar to complexes **1** and **2**, upon activation with 500 equiv of MAO complex, **3** gives rise to an active oligomerization catalyst which produces a distribution of soluble α-olefins along with some insoluble waxy polymers (ca. 15−20%). The activity of **3** (TON in ethylene of 10370) is somewhat lower than **1** and **2**, which give turnover numbers of (2−3) × 10^4 under comparable conditions ([Cr] = 200 μM, 5 bar ethylene, 30 min, see the Experimental Section). As we were primarily interested in oligomer selectivity, no attempt has been made to optimize

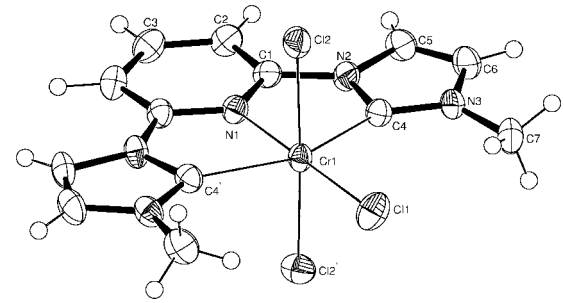

Figure 3. Molecular structure of **3**. Selected bond distances (Å) and angles (deg), together with corresponding parameters[43] for complex **1** in brackets: Cr1−C4 2.098(3) [2.120(6), 2.087(6)], Cr1−N1 2.058(3) [2.049(4)], Cr1−Cl1 2.2994(11) [2.2988(17)], Cr1−Cl2 2.3304(10) [2.3461(17), 2.3361(17)], N1−Cr1−C4 75.76(7) [76.3(2), 75.68(9)], C4−Cr1−C4′ 151.53(14) [154.9(2)] (′ denotes symmetry operator $-x$, y, $0.5-z$).

the activity of **3**. The C_8−C_{20} oligomers follow a Schulz−Flory distribution with a *K* value of 0.47, essentially the same as that found for **1**. The amounts of 1-butene and 1-hexene formed, however, are more like those of catalyst **2**. The 1-butene content is only 23% of that predicted from the Schulz−Flory distribution, while only 71% of the predicted 1-hexene is formed.

Oligomerization with a mix of CD_2CD_2/CH_2CH_2 reveals that this distribution is again the result of an extended metallacycle mechanism, as shown in Figure 4 which compares the predicted Cossee−Arlman and metallacycle isotopomer distributions for 1-decene against that observed experimentally. Agreement between the observed and predicted metallacycle distributions is generally good across the molecular weight range, while significant deviation from the Cossee−Arlman distribution is observed for around half of the molecular weights. It is interesting that complexes **2** and **3** lead to a similar reduction in 1-butene and 1-hexene formation, while **1** leads only to lower than expected 1-butene (and the reduction in 1-butene is much less pronounced than in **2** and **3**). Clearly, decomposition of the lower metallacycles (Cr−C_4, Cr−C_6) is more facile in **1** than in **2** and **3**. This does not follow a simple pattern of steric bulk at the ligand, as the isopropyl substitution in **1** is intermediate between **2** (2,6-diisopropylphenyl substitution) and **3** (methyl substitution). A more subtle ligand interaction with the metallacycle must be responsible, but lacking further insight at the molecular level we are unable to suggest what this might be.

Preparation and Oligomerization Studies of Cr(C^N)Cl_3(thf) (4). A range of bidentate phosphine ligands, in addition to well-known PNP ligands,[14] have been shown to catalyze the tetramerization of ethylene in combination with chromium.[50] We were therefore interested to explore the influence of bidentate ligands containing N-heterocyclic carbenes, given the known catalytic outcomes linking these ligand types. Theopold prepared chromium complexes of bidentate bis-carbenes and found that they displayed only low activity for ethylene polymerization.[51] Given the high activities of **1**−**3**, we have kept the C^N coordination mode and have prepared the pyridyl-carbene complex **4** according to Scheme 5. The course of this reaction was found to be highly dependent upon the rate

(50) Overett, M. J.; Blann, K.; Bollmann, A.; de Villiers, R.; Dixon, J. T.; Killian, E.; Maumela, M. C.; Maumela, H.; McGuinness, D. S.; Morgan, D. H.; Rucklidge, A.; Slawin, A. M. Z. *J. Mol. Catal. A* **2008**, *283*, 114.

(51) Kreisel, K. A.; Yap, G. P. A.; Theopold, K. H. *Organometallics* **2006**, *25*, 4670.

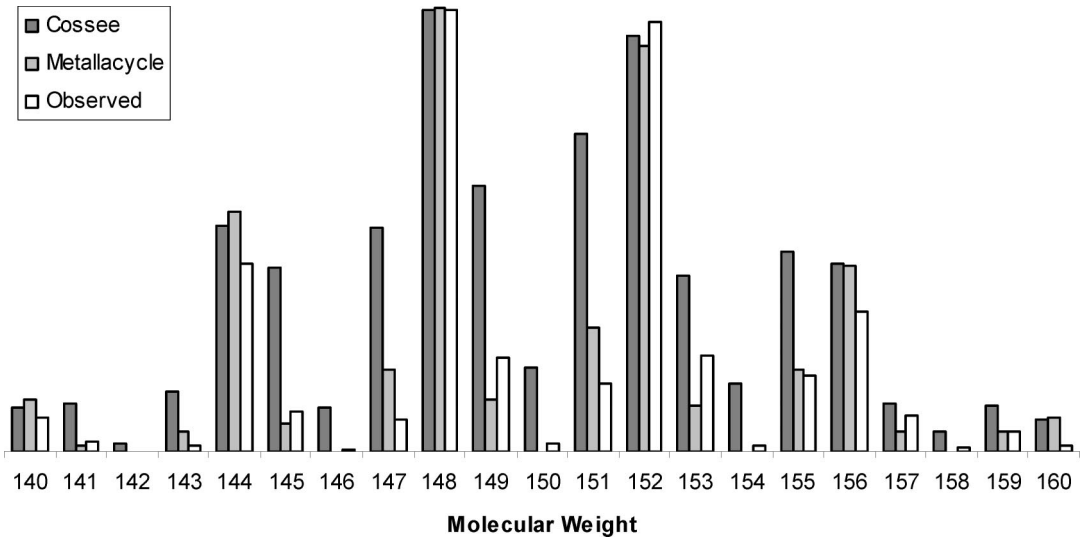

Figure 4. Predicted 1-decene isotopomer distribution for Cossee−Arlman and metallacycle mechanisms against the experimentally observed distribution for the catalyst system **3**/MAO.

Scheme 5. Preparation of Complexes 4 and 5 (Arbitrary Isomers Shown for Both)

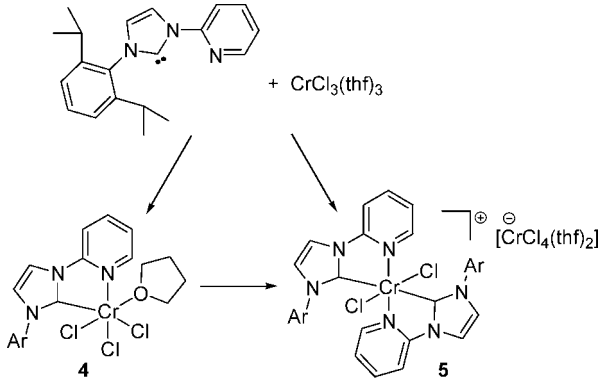

of addition of the carbene ligand to $CrCl_3(thf)_3$. When the ligand was added too rapidly, a large amount of highly insoluble pink precipitate was formed (complex **5**). By adding the ligand solution dropwise over one hour precipitation was kept to a minimum, and a soluble purple product (**4**) was obtained following filtration and removal of the solvent. Attempts to recrystallize **4** invariably lead to formation of **5**, at least in part, thus it proved difficult to obtain highly accurate elemental analyses or identification by a crystal structure determination. Nonetheless, elemental analysis along with high resolution mass spectroscopy support the formulations shown (see the Experimental Section). Recrystallization of **5** from acetonitrile apparently results in the formation of $[CrL_2Cl_2]Cl$ by elemental analysis and mass spectroscopy, supporting the notion that the cationic chromium center in **5** contains two C^N ligands.

Complex **5** did not lead to any ethylene oligomers when activated with MMAO-3A but instead gave a small amount of polyethylene corresponding to a turnover number in ethylene of 820. While **4** has a similar low activity (TON = 710 at 5 bar ethylene, 500 equiv of MMAO-3A), the results were somewhat more interesting. A Schulz−Flory distribution ($K = 0.76$) of even-carbon numbered oligomers resulted in which each carbon number fraction contained four different hydrocarbons. These were identified by GC−MS and consist of methyl-branched and linear paraffins and olefins as highlighted in Scheme 6. The C_{10} fraction, for instance, contained 13% 8-methyl-1-nonene, 25% 2-methylnonane, 20% 1-decene, and 42% *n*-decane. The

Scheme 6. Proposed Mechanism for the Formation of Linear/Branched Olefins and Paraffins via Linear Chain Growth/Chain Transfer

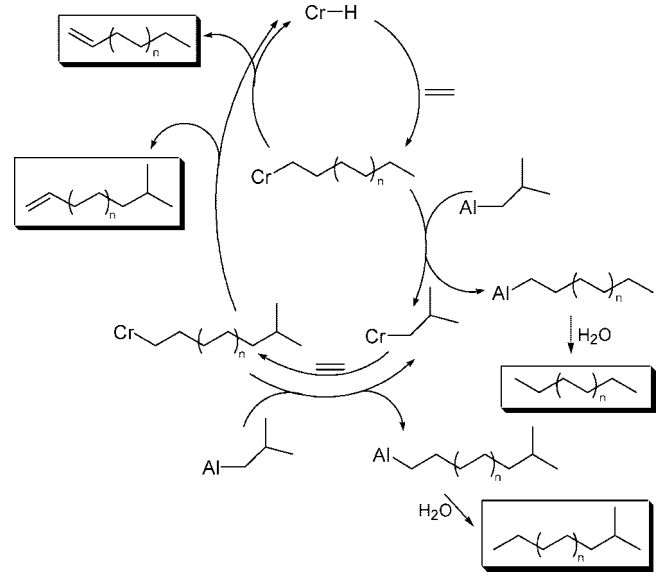

formation of oligomers with methyl branching in the 2-position can be accounted for by the incorporation of isobutyl groups from MMAO-3A into the oligomeric chain.[52] Scheme 6 shows the conventional mechanism by which this incorporation can occur, involving chain-transfer reactions with isobutylaluminum (assuming a Cossee−Arlman linear chain growth mechanism). However, given the established mode of oligomerization with **1**-**3**, we have also considered a metallacycle mechanism involving chain-transfer reactions (Scheme 7). In such a mechanism, chain transfer with an isobutylaluminum group would result in opening of the metallacycle (path a), from which a reductive β-hydrogen transfer from the isobutyl group would generate a Cr−isobutene complex and a linear aluminum alkyl (path b). Metallacycle formation from the Cr−isobutene complex (path c) would produce a dimethyl branched metallacycle, from which a methyl branched olefin could be released (path

(52) Akzo-Nobel MMAO-3A contains 30% Al^{i}Bu groups; nominal formula $[(CH_3)_{0.7}(^iC_4H_9)_{0.3}AlO]_n$.

Scheme 7. Proposed Mechanism for the Formation of Linear/Branched Olefins and Paraffins via a Metallacycle/Chain-Transfer Route

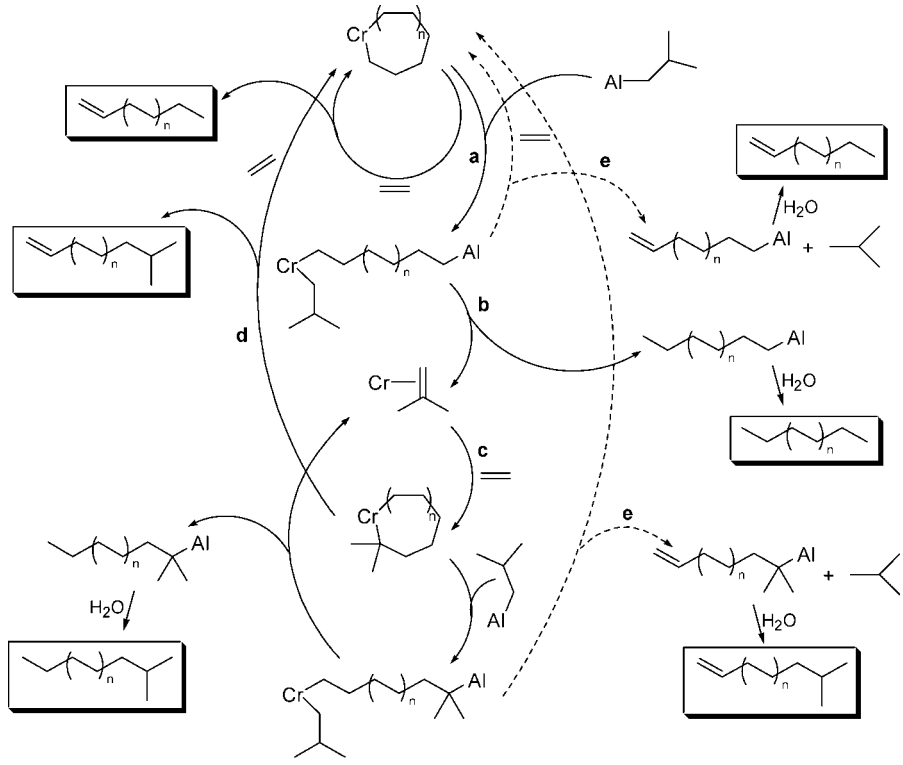

d). The linear and branched paraffins are produced from quenching of the aluminum alkyls formed by chain transfer. Also shown in Scheme 7 is a possible pathway to both olefins via aluminum species (path e), which involves β-hydrogen transfer from the oligomeric chain to the isobutyl group.

A number of investigations were carried out to determine the most likely mechanism. Quenching the reaction mixture with D_2O results in paraffins which are monodeuterated, supporting a chain transfer to aluminum mechanism, whether via Scheme 6 or Scheme 7. At the same time, the olefins contain no deutuerium, which precludes path e, Scheme 7, at the outset. The effect of increasing the pressure of ethylene also suggests that paraffin formation originates from chain transfer with aluminum. While the rate of oligomerization to olefins should be increased at higher ethylene pressure, the rate of chain transfer to aluminum should be unaffected. Consistent with this, a 30 min catalytic run conducted at 30 bar of ethylene resulted in a 4-fold increase in olefin formation relative to the run at 5 bar (with most of this coming from an increase in linear α-olefins), while the amount of paraffins remained relatively unaffected.

A number of additional experiments indicated that a metallacycle mechanism is not operating. Careful analysis of the C_4 fraction failed to detect any isobutene. It would be expected that at least traces of this would be present if a Cr-*iso*-butene complex forms as in Scheme 7. Additionally, when isobutene was added to an oligomerization run no incorporation occurred. The most definitive evidence for a linear chain growth mechanism with this catalyst comes from oligomerization with a mix of CD_2CD_2/CH_2CH_2, which reveals deuterium scrambling in the olefins. This is clearly seen in the 4-methyl-1-pentene formed, which only contains the d_3 isotopomer in addition to the nondeuterated isotopomer. As shown in Scheme 8, a metallacycle mechanism would yield a d_4 isotopomer, while insertion of CD_2CD_2 into a Cr−isobutyl group would yield 4-methyl-1-pentene-d_3, as observed.[53]

Scheme 8

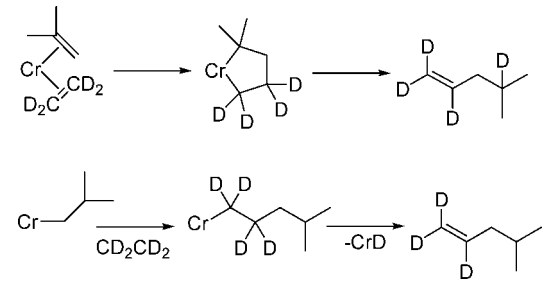

Preparation and Oligomerization Studies of Thienyl−Carbene Chromium Complexes 6 and 7. Among the ligands known to promote chromium-catalyzed ethylene trimerization, tridentates containing sulfur in combination with other donors (N, P) have been shown to be particularly effective in cases.[7,11,54] With this in mind, we prepared complex **6** according to Scheme 9, which contains a central thiophene donor group while maintaining structural similarity to the CNC ligands in **1**−**3**. The free carbene ligand was found to be highly unstable, and attempts to isolate it by removal of the solvent (THF) resulted in decomposition to a black tar. However, by reacting the ligand with $CrCl_3(thf)_3$ immediately after generation of the carbene, complex **6** was formed in high yield. Disappointingly, the combination of **6**/MAO did not lead to any oligomerization even at ethylene pressures up to 30 bar. Some trace polymer appeared to form, but this was not enough to quantify. Clearly, the central pyridyl donor group in **1**−**3** plays a crucial role in catalysis, while its replacement with a thiophene group has

(53) In the linear chain growth mechanism of Scheme 8, chain termination is shown as proceeding via β-D elimination. Alternatively, it could also occur via a concerted β-D transfer to ethylene, which would yield the same result.

(54) McGuinness, D. S.; Wasserscheid, P.; Morgan, D. H.; Dixon, J. T. *Organometallics* **2005**, *24*, 552.

Scheme 9. Preparation of Complex 6

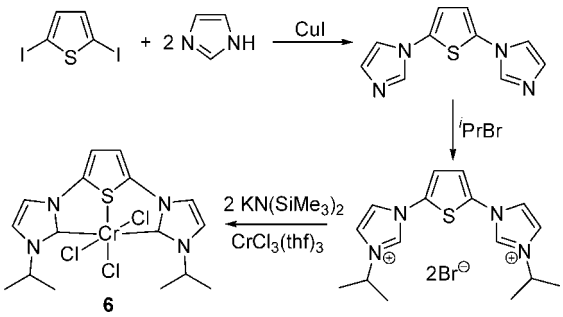

created a ligand which is essentially a very effective poison to chromium.[55]

The bidendate version of the C^S^C ligand featured in complex **6** was prepared and reacted with $CrCl_3(thf)_3$ to yield complex **7** (reaction 2). The free carbene is more stable in this instance and could be isolated. Upon reaction with $CrCl_3(thf)_3$, either $CrLCl_3(thf)$ (in analogy to **4**) or the dimer $[CrLCl_2(\mu\text{-}Cl)]_2$ were expected, both of which would maintain the favored hexacoordination of chromium(III). The pink product which was isolated analyzed as being midway between these ($CrLCl_3(thf)_{0.5}$). While we were unable to obtain crystals for a structural determination, it seems possible that tetrahydrofuran is partially removed from $CrLCl_3(thf)$ when the solvent is removed under vacuum. The exact nature of this complex remains uncertain. When tested under standard conditions with MAO cocatalyst, complex **7** produced 77% polyethylene and 23% soluble oligomers with rather low activity (TON in ethylene = 1030). The liquid fraction was made up of a main Schulz−Flory distribution ($K = 0.35$) of even carbon numbered α-olefins (80%) and paraffins (20%). A second distribution of odd carbon numbered olefins and paraffins with the same K value was also present (20% relative to the main distribution), indicating chain transfer with Al-Me is significant. These observations suggest that the modest activity for polymerization with **7** results form a linear chain growth mechanism, in analogy to **4**.

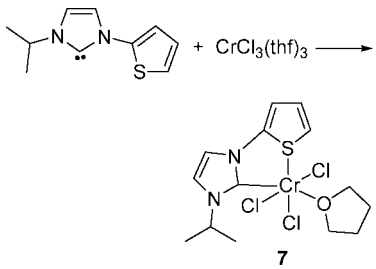

3. Summary and Conclusion

This work has shown that chromium complexes of bis(carbene)pyridine ligands catalyze the oligomerization of ethylene via a metallacycle mechanism and have revealed further insights into extended metallacycle growth. First, significant deviation from a Schulz−Flory distribution of oligomers has been found, indicating that the product releasing metallacycle decomposition is retarded relative to further growth at the Cr−C_4 (±Cr−C_6) stage. This is partly influenced by substitution at the carbene nitrogen centers, with the effect being most pronounced with catalysts **2** and **3**, which also lead to reduced 1-hexene formation. The results also indicate that metallacycle decomposition occurs from chromium species in which an interaction with additional ethylene must be present, as increased ethylene pressure does not affect the oligomer distribution. Thus, the rates of ethylene insertion and metallacycle decomposition are both increased to the same degree when the concentration of monomer increases. Incorporation of preformed α-olefins into the metallacycle structure has been demonstrated, and results in co-oligomerization of ethylene with the α-olefins. This process produces small amounts of both methylidenes and linear internal olefins along with the main distribution of α-olefins.

Modification of the C^N^C ligand structure did not lead to any improvement in either activity or olefin selectivity. To the contrary, bidentate carbene−pyridine and carbene−thiophene ligands led to very low activity for ethylene oligomerization, while the tridentate bis(carbene) thiophene complex **6** led to no detectable activity. The change to a bidentate ligand structure in complexes **4** and **7** led to a switch in the mechanism of oligomer growth, from metallacycle to Cossee−Arlman type chain growth. It is an interesting observation that a metallacycle mechanism results in very high activity, while the switch to linear chain growth is accompanied by very poor activity. Previous work has shown that a number of other highly active chromium-based systems operate via an extended metallacycle mechanism,[33,34] and this work demonstrates yet another example of this. Further work is required to investigate just how general this mechanism is in chromium catalyzed ethylene oligomerization and polymerization.

4. Experimental Section

4.1. General Comments. All manipulations were carried out using standard Schlenk techniques or in a nitrogen glovebox using solvents purified by passage through an Innovative Technologies solvent purification system (purification over activated alumina, copper catalyst, and/or molecular sieves). Ethylene was purified by passage through activated 3 Å molecular sieves followed by alumina. Complexes **1** and **2** were prepared as reported previously.[43] The C^N ligand, 1-(2,6-diisopropylphenyl)-3-pyridylimidazol-2-ylidene, has been reported previously.[56] ^1H and ^{13}C NMR spectra were recorded on a Varian Mercury Plus NMR spectrometer operating at 300 and 75 MHz, respectively, with spectra referenced against residual solvent peaks (^1H NMR) or to the ^{13}C resonances of the solvent.

Liquid secondary ion MS (LSIMS) analyses were carried out on a Kratos ISQ mass spectrometer using a primary beam of Cs ions at 10 kV. Samples were dissolved in *m*-nitrobenzyl alcohol (mnba), and the secondary ions formed accelerated at 5.3 kV. Accurate masses were determined by peak matching at a resolution of 7000 using mnba and CsI/PEG multimers as reference masses. Electrospray mass spectra were recorded on a Finnigan LCQ ion trap by direct infusion of the sample dissolved in methanol.

GC−MS analyses were carried out on a Varian 3800 GC coupled to Varian 1200 triple quadrupole mass spectrometer in single quadrupole mode. The column was a Varian "Factor Four" VF-5 ms (30 m × 0.25 mm internal diameter and 0.25 μm film). Injections of 1 μL of diluted samples were made using a Varian CP-8400 autosampler and a Varian 1177 split/splitless injector with a split ratio of 20:1. The ion source was at 230 °C, and the transfer line at 290 °C. The carrier gas was helium at 1.2 mL per minute using constant flow mode. The injector temperature was 220 °C. For Figure S4 (Supporting Information), the column oven was held

(55) It has been shown previously that $CrCl_3(thf)_3$ without additional ligation is a very effective ethylene oligomerization catalyst in combination with MAO. McGuinness, D. S.; Overett, M.; Tooze, R. P.; Blann, K.; Dixon, J. T.; Slawin, A. M. Z. *Organometallics* **2007**, *26*, 1108.

(56) Winston, S.; Stylianides, N.; Tulloch, A. A. D.; Wright, J. A.; Danopoulos, A. A. *Polyhedron* **2004**, *23*, 2813.

at 40 °C for 2 min then ramped to 290 °C at 15 degrees per min. For Figure S5 (Supporting Information), the column oven was held at 50 °C for 2 min and then ramped to 290 °C at 8 °C/min. The range from *m*/*z* 35 to 450 was scanned 4 times/s.

Uncorrected isotopomer ratios were determined for the C10 oligomer by plotting chromatograms for every ion between *m*/*z* 140 and *m*/*z* 160 inclusive and measuring the 1-decene peak area. GC retention times for each isotopomer decreased as expected with increasing levels of deuterium incorporation. Corrections for naturally occurring isotopes of C and H and for isotopic impurities in the CD_2CD_2 were then made (see the Supporting Information for further details).

4.2. Structural Determination of Complex 3. Data were collected at 193 K with an Enraf-Nonius TurboCAD4 with Mo-K_α radiation, (0.71073 Å) on prismatic crystals of [(2,6-{$MeC_3N_2H_2$}C_5NH_3)$CrCl_3$].2CH_2Cl_2 **3**, belonging to the space group *C*2/*c* (No. 15). A summary of crystallographic data, data collection parameters, and refinement parameters are given below. The structure was solved by direct methods with SHELXS97, refined using full-matrix least-squares routines against F^2 with SHELXL97,[57] and visualized using X-SEED.[58]

The asymmetric unit of the structure contains one-half of a molecule of complex **3** residing on a 2-fold crystallographic rotation axis (0,*y*,0.25: containing C3, N1, Cr1, and Cl1) and one solvent molecule of dichloromethane. The molecular symmetry of complex **3** approximates to C_{2v}, with the largest deviations toward the lower crystallographic symmetry relating to the conformations of the methyl groups. A disorder in the solvent molecule was apparent in Fourier maps and was modeled as a two-site occupancy disorder limited to one of the Cl centers (and the methylene protons in consequence) having refined occupancies of 0.718(8) (Cl4A) and its complementary (Cl4B). Structure refinement in various space groups yielded the same disorder, with no improvements in the disorder model and/or residuals. Data were collected on several crystals, with similar disorder outcomes. Thus, refinement in the highest symmetry space group matching the observed systematic data absences is presented. All non-hydrogen atom positions of the complex and solvent molecules were refined anisotropically. All hydrogens of the complex were located and refined (x,y,z,U_{iso}), while those on the disordered solvent molecule were included in calculated positions with a "riding" model with C−H distances of 0.99 Å and with $U_{iso}(H) = 1.2U_{eq}(C)$.

Crystal data for 3: $C_{15}H_{17}Cl_7CrN_5$, $M = 567.49$, green prism, $0.45 \times 0.25 \times 0.15$ mm^3, monoclinic, space group *C*2/*c* (No. 15), $a = 14.649(5)$ Å, $b = 14.395(3)$ Å, $c = 11.144(8)$ Å, $\beta = 107.51(4)°$, $V = 2241.1(19)$ Å^3, $Z = 4$, $D_c = 1.682$ g/cm^3, $F_{000} = 1140$, Enraf-Nonius TurboCAD4, Mo Kα radiation, $\lambda = 0.71073$ Å, $T = 193(2)$ K, 2093 reflections collected, 1983 unique ($R_{int} = 0.0321$). Final GooF = 1.094, R1 = 0.0339, wR2 = 0.0881, *R* indices based on 1714 reflections with $I > 2\sigma(I)$ (refinement on F^2), 165 parameters, 0 restraints. Lp and absorption (analytical) corrections applied, $\mu = 1.358$ mm^{-1}.

4.3. Ethylene Oligomerization. In a standard ethylene oligomerization run, a 300 mL Lab-Crest glass reactor was put under an ethylene atmosphere by successive pressure/purge cycles and charged with toluene such that the final volume in the reactor was 50 mL. The chromium-based catalyst (10 μmol) was dissolved/suspended in toluene and added to the reactor, followed by 500 equivalents of MAO (or MMAO-3A) solution. The reactor was immediately pressurized with ethylene to 4 bar gauge (5 bar absolute) and maintained within 1 degree of 25 °C by periodic cooling in a water bath. After 30 min the ethylene supply was stopped and the reactor cooled to around 0 °C. Excess ethylene was vented and collected in a Teflon gas bag for analysis. Nonane (internal standard, 1000 μL) was added before quenching the reactor contents with 10% HCl. A sample of the organic phase was analyzed by GC-FID, while the solids from the bulk of the solution were collected by filtration, washed with ethanol, dried, and weighed. Higher pressure runs were conducted similarly in a Parr 300 mL stainless steel reactor.

4.4. Synthesis of Compounds. 2,6-Bis(1-methylimidazolium)pyridine Dibromide. A mixture of 2,6-dibromopyridine (2.09 g, 8.82 mmol) and *N*-methylimidazole (2 mL, 25 mmol) was put under argon and heated to 170 °C overnight. Upon cooling, the solid was broken up and triturated with 10 mL of methylene chloride until a fine powder formed. THF (10 mL) was added and the solvent filtered off. The remaining solid was washed twice with THF (10 mL) and dried under vacuum to give a colorless powder. Yield: 3.26 g (92%). ^{1}H NMR (300 MHz, DMSO-d_6): δ 4.03(s, 6H, NCH_3); 8.06 (s, 2H, NC(*H*)C(H)N); 8.22 (d, $J = 8$ Hz, 2H, 4,6-py*H*); 8.59 (t, $J = 8$ Hz, 1H, 5-py*H*); 8.80 (s, 2H, NC(H)C(*H*)N); 10.61 (s, 2H, NC(*H*)N). ^{13}C NMR (75 MHz, DMSO-d_6): δ 37.2 (*C*H_3); 114.7, 137.0, 145.6 (py*C*); 119.8, 125.7 (N*CC*N); 145.9 (N*C*N). MS (LSIMS): *m*/*z* 240 [M − H]$^+$; 320 [M + Br]$^+$.

2,5-Bis(1-isopropylimidazolium)thiophene Dibromide. A Schlenk flask was charged with 2,5-diiodothiophene (5.55 g, 16.5 mmol), imidazole (2.32 g, 34.1 mmol), Cs_2CO3 (10.11 g, 31 mmol), CuI (0.56 g), and 1,10-phenanthroline (0.53 g) and put under argon. Dry DMF (20 mL) was added and the mixture heated to 130 °C for 4 days. Methylene chloride (20 mL) was added, and the solution was extracted three times with water (ca. 80 mL total). Methylene chloride was removed from the organic phase, and the residue was flash distilled under full oil pump vacuum. Residual DMF which distilled off at 60−70 °C was discarded and the oil distilling at 170−200 °C was collected. To this was added isopropyl bromide (5 mL, 53 mmol), and the solution was heated to 90 °C for 2 days. Upon cooling, a sticky solid resulted which was washed with methylene chloride (3 × 5 mL) to give a colorless powder. Yield: 1.25 g (16%). ^{1}H NMR (300 MHz, DMSO-d_6): δ 1.54 (d, $J = 7$ Hz, 12H, CH_3); 4.76 (m, $J = 7$ Hz, 2H, C*H*(CH_3)$_2$); 7.69 (s, 2H, thiophene-*H*); 8.24 (s, 2H, NC(*H*)C(H)N); 8.29 (s, 2H, NC(H)C(*H*)N); 9.97 (s, 2H, NC(*H*)N). ^{13}C NMR (75 MHz, DMSO-d_6): δ 22.8 (*C*H_3); 53.8 (*C*(CH_3)$_2$); 122.1, 134.3 (thiophene-*C*); 123.6, 124.1 (N*CC*N); 137.1 (N*C*N). MS (LSIMS): *m*/*z* 301 [M − H]$^+$; 381 [M + Br]$^+$.

1-Isopropyl-3-thienylimidazolium Bromide. *N*-tThienylimidazole (0.615 g, 4.09 mmol) and 2-bromopropane (0.80 mL, 8.4 mmol) were put under argon in a Schlenk flask and heated to 110 °C overnight. The glasslike solid that formed upon cooling was taken up in methylene chloride (4 mL), and THF was added dropwise until the solution went persistently cloudy. After a short time, a colorless precipitate formed. The solvent was decanted off and the product washed three times with THF (10 mL). Yield: 0.964 g (86%). ^{1}H NMR (300 MHz, DMSO-d_6): δ 1.52 (d, $J = 7$ Hz; 6H, CH_3); 4.71 (m, $J = 7$ Hz, 1H, C*H*(CH_3)$_2$); 7.15 (dd, $J = 4$ Hz, 6 Hz, 1H, 4-thiophenyl-*H*); 7.59 (d, $J = 4$ Hz, 1H, thiophenyl-*H*); 7.66 (d, $J = 6$ Hz, 1H, thiophenyl-*H*); 8.19 (s, 1H, NC(*H*)C(H)N); 8.26 (s, 1H, NC(H)C(*H*)N); 9.86 (s, 1H, NC(*H*)N). ^{13}C NMR (75 MHz, DMSO-d_6): δ 22.2 (*C*H_3); 53.0 (*C*(CH_3)$_2$); 121.5, 122.8, 123.0, 125,7, 126.7 (thiophene-*C* and N*CC*N); 135.4 (N*C*N). MS (ESI): *m*/*z* 193 [M]$^+$; 151 [M − propene]$^+$.

2,6-Bis(1-methylimidazol-2-ylidene)pyridine. A mixture of 2,6-bis(1-methylimidazolium)pyridine dibromide (1.575 g, 3.93 mmol) and KN($SiMe_3$)$_2$ (1.64 g, 8.22 mmol) was cooled to −15 °C and THF (20 mL) added. The solution was allowed to slowly warm to room temperature and stir overnight. Filtration gave a deep red-brown solution from which the solvent was removed to leave an oil. This was washed with hexane/Et_2O (5 mL/5 mL), followed by cold Et_2O (−20 °C, 2 × 10 mL) to afford a rust brown powder. Yield: 0.490 g (52%). ^{1}H NMR (300 MHz, C_6D_6): δ 3.33 (s, 6H,

(57) Sheldrick, G. M. *SHELX97 Programs for Crystal Structure Analysis*; Universität Göttingen: Germany, 1998.

(58) Barbour, L. J. J. *J. Supramol. Chem.* **2001**, *1*, 189.

NC*H*$_3$); 6.27 (d, J = 1.8 Hz, 2H, NC(*H*)C(H)N); 7.11 (t, J = 7.8 Hz, 1H, 4-py*H*); 7.89 (d, J = 1.8 Hz, 2H, NC(H)C(*H*)N); 8.40 (d, J = 7.8 Hz, 2H, 3,5-py*H*). ^{13}C NMR (75 MHz, C_6D_6): δ 37.9 (N*C*H$_3$); 110.9, 120.4 (N*CC*N); 116.5, 140.4, 152.6 (py*C*); 217.3 (N*C*N).

2,5-Bis(1-isopropylimidazol-2-ylidene)thiophene. 2,5-Bis(1-isopropylimidazolium)thiophene dibromide (0.111 g, 0.240 mmol) was suspended in THF (10 mL) and cooled to −10 °C. A solution of KN(SiMe$_3$)$_2$ (0.099 g, 0.50 mmol) in 5 mL of THF was slowly added, and the mixture was allowed to warm to room temperature. After being stirred for 1 h, the solution was filtered and the solvent removed under vacuum. The solution darkened considerably as the THF was removed, finally going black as it was taken to dryness. While most of this decomposed material was insoluble in C_6D_6, that which did dissolve gave a proton NMR spectrum consistent with the free carbene. ^{1}H NMR (300 MHz, C_6D_6): δ 1.14 (d, J = 6.6 Hz, 12H, NC*H*$_3$); 4.19 (m, J = 6.6 Hz, 2H, C*H*(CH$_3$)$_2$); 6.29 (s, 2H, thiophene*H*); 6.47 (s, 2H, NC(*H*)C(H)N); 6.79 (s, 2H, NC(H)C(*H*)N).

1-Isopropyl-3-thienylimidazol-2-ylidene. 1-Isopropyl-3-thienylimidazolium bromide (0.964 g, 3.53 mmol) was suspended in 5 mL of THF at −20 °C. To this was added a solution of KN(SiMe$_3$)$_2$ (0.743 g, 3.72 mmol) in 10 mL of THF. The mixture was allowed to warm to room temperature and then stirred for 1 h. After filtration, the solvent was removed to leave an oil. This was washed with hexane/Et$_2$O (5 mL/2 mL) at −40 °C to slowly give a powder, which was washed with further hexane at −40 °C (3 × 5 mL). Drying under vacuum gave a light gray powder. Yield: 0.576 g (85%). ^{1}H NMR (300 MHz, C_6D_6): δ 1.14 (d, J = 7 Hz; 6H, C*H*$_3$); 4.21 (m, J = 7 Hz, 1H, C*H*(CH$_3$)$_2$); 6.30 (d, J = 1.5 Hz, 1H, NC(*H*)C(H)N); 6.38 (d, J = 5 Hz, 1H, thiophenyl-*H*); 6.54 (dd, J = 4 Hz, 5 Hz, 1H, 4-thiophenyl-*H*); 6.80 (d, J = 1.5 Hz, 1H, NC(H)C(*H*)N). ^{13}C NMR (75 MHz, C_6D_6): δ 23.8 (*C*H$_3$); 52.4 (*C*(CH$_3$)$_2$); 112.0, 116.9, 117.4, 119.0 (N*CC*N and thienyl*C*); 125.3 (NC*C*N); 147.7 (thienylC_{ipso}); 215.0 (N*C*N).

2,6-Bis(1-methylimidazol-2-ylidene)pyridine Chromium Trichloride (3). A solution of the free carbene (0.127 g, 0.531 mmol) in 7 mL of THF was slowly added to a solution of CrCl$_3$(thf)$_3$ (0.180 g, 0.480 mmol) in 13 mL of THF, leading to the instantaneous formation of a green precipitate. This was stirred for 1 h before the solvent was filtered off and the precipitate washed with 20 mL of THF followed by 10 mL of methylene chloride. Drying under vacuum gave a green powder. Yield: 0.191 g (100%). Crystals suitable for X-ray diffraction analysis were grown by vapor diffusion of methylene chloride into a DMSO solution. MS (LSIMS): m/z 361 [CrLCl$_2$]$^+$; 326 [CrLCl]$^+$; 291 [CrL]$^+$. Anal. Calcd for $C_{13}H_{13}N_5CrCl_3 \cdot CH_2Cl_2$ (found): C, 38.24 (38.25); H, 3.26 (3.52); N, 16.89 (16.86).

1-(2,6-Diisopropylphenyl)-3-pyridylimidazol-2-ylidenetetrahydrofuran Chromium Trichloride (4). A solution of CrCl$_3$(thf)$_3$ (0.250 g, 0.667 mmol) in 15 mL of THF was treated dropwise with a solution of the free carbene (0.204 g, 0.668 mmol) in 5 mL of THF. The rate of addition (ca. 1 h) was such that precipitation was kept to a minimum, with a pink precipitate forming permanently toward the end of the addition. The dark purple solution was filtered from the precipitate into a second Schlenk flask. The precipitate was washed with THF and dried under vacuum to give a light pink powder formulated as [CrL$_2$Cl$_2$][CrCl$_4$(thf)$_2$] (**5**). Yield: 0.101 g (28%). Anal. Calcd for $C_{48}H_{62}N_6O_2Cr_2Cl_6$ (found): C 53.79 (53.21); H, 5.83 (5.49); N, 7.84 (8.30). HRMS (LSIMS): m/z calcd for [L$_2$CrCl$_2$]$^+$ (found) 732.256610 (732.25681). The only signal observed in the negative ion mass spectrum was a cluster at 863, corresponding to [Cr$_3$Cl$_6$(thf)$_4$]$^-$ and presumably resulting from oligomerization of the anion in the mass spectrometer. The mother liquor from the original reaction mixture was reduced until ca. 3 mL remained and Et$_2$O was added (5 mL), causing the product to drop out of solution. The solution was filtered and the precipitate washed with Et$_2$O and dried under vacuum to give a purple powder, CrLCl$_3$(thf) (**4**). Yield: 0.227 g (63%). Anal. Calcd for $C_{24}H_{31}N_3OCrCl_3$ (found): C, 53.79 (54.44); H, 5.83 (5.83); N, 7.84 (7.20). HRMS (LSIMS): m/z calcd. for [LCrCl$_2$]$^+$ (found) 427.067420 (427.06624).

2,5-Bis(1-isopropylimidazol-2-ylidene)thiophene Chromium Trichloride (6). A THF solution of the free carbene was prepared as described above from 2,5-bis(1-isopropylimidazolium)thiophene dibromide (0.0972 g, 0.210 mmol) and KN(SiMe$_3$)$_2$ (0.091 g, 0.456 mmol). This was filtered into a solution of CrCl$_3$(thf)$_3$ (0.073 g, 0.19 mmol) in 5 mL of THF, giving a green precipitate immediately. After the mixture was stirred overnight the solvent was filtered off, and the precipitate washed with THF (2 × 10 mL) and dried under vacuum to give a green powder. Recrystallization from DMSO/methylene chloride gave a microcrystalline solid. Yield: 0.0806 g (92%). MS (LSIMS): m/z 301 [LH]$^+$. Anal. Calcd for $C_{16}H_{20}N_4SCrCl_3 \cdot$DMSO (found): C, 40.27 (40.62); H, 4.88 (5.35); N, 10.44 (10.68).

1-Isopropyl-3-thienylimidazol-2-ylidene Chromium Trichloride · $^1/_2$Tetrahydrofuran (7). A solution of the free carbene (0.111 g, 0.577 mmol) in 5 mL of THF was added to a solution of CrCl$_3$(thf)$_3$ (0.202 g, 0.539 mmol) in 10 mL of THF. The solution was stirred for 1 h before being filtered to remove trace dark solid (carbene decomposition product). The solvent was removed from the filtrate until a slurry formed, and 5 mL of Et$_2$O was added to complete precipitation. After washing with Et$_2$O (2 × 10 mL), the solid was dried under vacuum to give a pink powder. Yield: 0.221 g (94%). Anal. Calcd for $C_{12}H_{16}N_2SO_{0.5}CrCl_3$ (found): C, 37.27 (37.14); S, 8.29 (8.35); N, 7.24 (7.05); H, 4.17 (5.10). MS (LSIMS): m/z 506 [CrL$_2$Cl$_2$]$^+$; 471 [CrL$_2$Cl]$^+$; 314 [CrLCl$_2$]$^+$; 279 [CrLCl]$^+$; 193 [LH]$^+$.

Acknowledgment. We thank Albemarle Asia Pacific for donating MAO solution and Tony Caselli of Plastral Pty Ltd. for facilitating this. Marshall Hughes and Thomas Rodemann are thanked for acquisition of LSIMS data and elemental analyses, respectively. The Australian Research Council is thanked for financial support and a QEII Fellowship to D.S.M.

Supporting Information Available: X-ray crystallographic file (CIF) for **3**. Details of 1-decene isotopomer analysis and α-olefin incorporation product analysis. This material is available free of charge via the Internet at http://pubs.acs.org.

OM800398E